encit 2020

ABCM Associação Brasileira de Engenharia e Ciências Mecânicas

18th Brazilian Congress of Thermal Sciences and Engineering
November 16–20, 2020 (Online)

ENC-2020-0740
METHODOLOGY TO EVALUATE THE ACCURACY OF THERMAL CAMERAS NON-UNIFORMITY CORRECTION USING RAW DATA AND A BLACKBODY RADIATOR

Vitor F. Paes
Rafael A. M. Ferreira
Matheus P. Porto
Laboratório de Termometria - LabTerm, Programa de Pós-Graduação em Engenharia Mecânica, Escola de Engenharia, Universidade Federal de Minas Gerais, Belo Horizonte, MG, Brasil
matheusporto@ufmg.br

Abstract. *Herein we introduce a novel methodology to estimate the measurement uncertainty of thermal imagers due to the non-uniformity correction (NUC) procedure. NUC technique is largely discussed in the literature, on the other hand, its metrological accuracy is not so often debated. NUC is the most important step during the calibration of thermal imagers, and it corrects the precision of each pixel in the matrix. Despite being an efficient method to mitigate spatial noise (spatial precision), the NUC method does not provide a temperature correction, thus it must be made in a similar fashion as for the calibration of thermocouples. The scientific community fails not providing a gold standard method to relate non-uniformity correction procedures with temperature uncertainty. In this study, we introduce a novel method to mitigate the aforementioned issues, proposing to evaluate the uncertainties of the traditional two-point NUC using raw data and a blackbody radiator as the reference source. Three thermal imagers were tested under controlled conditions and the results for the performance evaluation of the NUC model show that the two-point NUC technique is an efficient method to reduce spatial noise in a narrow range of operation. The uncertainty propagation showed that the components related to the blackbody radiator were dominant in the proposed model, followed by the standard deviation and correction model uncertainties. To fully categorize the uncertainties in the correction model, a further examination of the thermal imager components must be made, considering the spectral response, intrinsic errors and detector's self emission.*

Keywords: *Infrared Thermography, Non-uniformity Correction, Uncertainty Propagation*

1. INTRODUCTION

Spatial non-uniformity in thermal images is the most relevant aspect regarding the thermal imager operation. These non-uniformity arise during manufacturing process and camera operation, when electronic noise disturbs the detector response into becoming non-homogeneous, which decreases the quality of the measurement (Poncelet and Witz, 2011; Saux and Doudard, 2016; Nelson *et al.*, 1991). To balance detector's response, a correction procedure is necessary. These methods are called non-uniformity corrections (NUC), divided into two categories consisting of reference-based techniques (Chang and Li, 2019; Li *et al.*, 2017; Miao *et al.*, 2009) and scene-based techniques (Rui *et al.*, 2009; Redlich *et al.*, 2015; Zhou *et al.*, 2009). These traditional procedures are often categorized as calibration techniques and are mostly done by the camera's manufacturer, but the calibration certificates issued lack key information about the methodological process, making the correction unrepeatable. Also, the evaluation of accuracy and performance of NUC procedures in the literature fail to provide an uncertainty analysis which is crucial for the comparison and validation of the methodology (Machin *et al.*, 2008; NISTIR, 2015).

Several studies investigated the performance and accuracy of non-uniformity techniques in thermal imagers. Chang and Li (2019) proposed a linear model for the correction of detector response applying a reference-based technique to compare the performance of the single-point and two-point NUC. Saux and Doudard (2016) presented a novel NUC methodology that evaluated the influence of operating temperature in the correction procedure. The performance of the novel correction and the traditional two-point NUC were compared. Miao *et al.* (2009) implemented a real-time multi-point NUC for short wave infrared focal plane array (IRFPA) and compared the performance with the two-point NUC.

These studies investigated the accuracy of correction techniques but they fail to provide an uncertainty analysis of the procedure. The objective of this study is to propose a methodology to evaluate the accuracy of the traditional two-point NUC using raw data and a blackbody radiator, taking into account the propagation of measurement uncertainties. We conducted experiments under controlled conditions using a blackbody radiator as the uniform source of radiation and raw data extracted from a thermal camera facing the reference source. Three similar cameras were used in the experiments

and a comparison between cameras is exposed in the results section.

This document is divided into the following sections: Section 2 describes the signal processing of a thermal camera and the nature of the raw data; Section 3 contains the mathematical model for the two-point NUC, the experimental procedure and the model for uncertainty propagation; Section 4 contains the results of the correction procedure and measurement uncertainties and Section 5 contains the concluding remarks.

2. SIGNAL PROCESSING AND RAW DATA

The signal processing in thermal cameras, independently of the type of the sensor (i.e., thermal or photonic), is done in a similar way. The incident radiation is refracted by the lens to the detector's array which generates an analog signal proportional to the radiant flux. The signal passes by an analog-digital module that converts the analog signal to a digital one, followed by a NUC procedure and a bad pixel replacement (BPR) that corrects each pixel response and regulate defective pixels. Finally, the digital signal is converted into temperature that is visually represented on the camera's display, according to a selected color scale. Figure 1 illustrates the signal processing in a thermal camera.

The digital signal array, obtained after the conversion process in the A/D module, is the most relevant data used in the correction procedures. The raw data correlates with the incident radiation flux received by each pixel and is the initial data used to obtain the correction coefficients and the corrected response. In this study, the raw data used on the thermal cameras correction was obtained directly by the imagers during the experimental procedure.

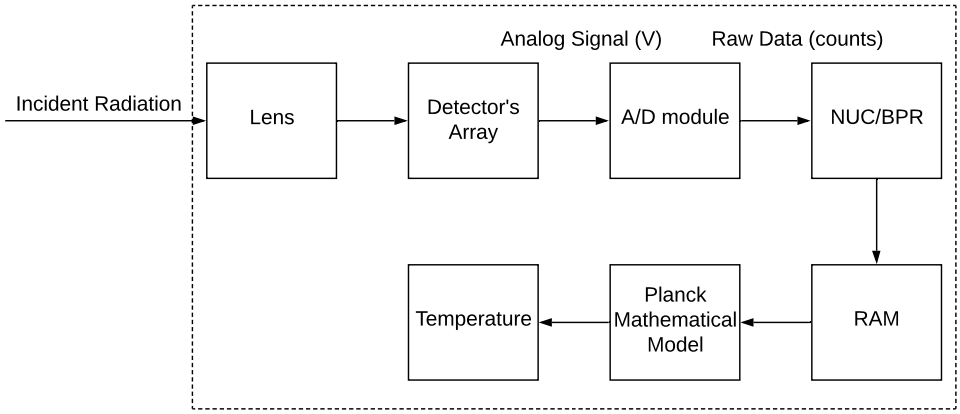

Figure 1: Sketch of a conventional thermal camera signal processing. Adapted from Honorat *et al.* (2005)

3. METHODOLOGY

The methodology of this study is divided into three subsections: NUC mathematical model, experimental procedure and uncertainties propagation.

3.1 NUC Mathematical Model

Traditional NUC models are based on the principle that the detectors exposed to a uniform radiation flux should return the same value of temperature. However, due to spatial non-uniformity, a non-homogeneous response is obtained which degrades radiometric measurement. The goal of the NUC model is to obtain the correction coefficients (gain and offset) and apply them into the original array to balance detector's response. The methodology diagram is presented in Fig. 2.

First, we propose a linear model to correlate each detector response to an incident radiation flux, described by Eq. 1.

$$Y_{ij} = G_{ij}X + O_{ij} \tag{1}$$

where Y_{ij} is the pixel response, G_{ij} is the gain coefficient, X is the incident radiation and O_{ij} is the offset coefficient. These raw data will be obtained for each reference temperature applied to the blackbody, analyzed in the approximated operation range of 30 ^oC to 45 ^oC.

In a thermography inspection, the incident radiation on the sensors consists of the energy emitted and reflected by the object surface and the energy emitted by the atmosphere between the camera and the inspected object. The total incident radiation is formulated according to Eq. 2.

$$S_{total} = \tau\epsilon_{obj}S_{obj} + \tau\left(1-\epsilon_{obj}\right)S_{refl} + \left(1-\tau\right)S_{atm} \tag{2}$$

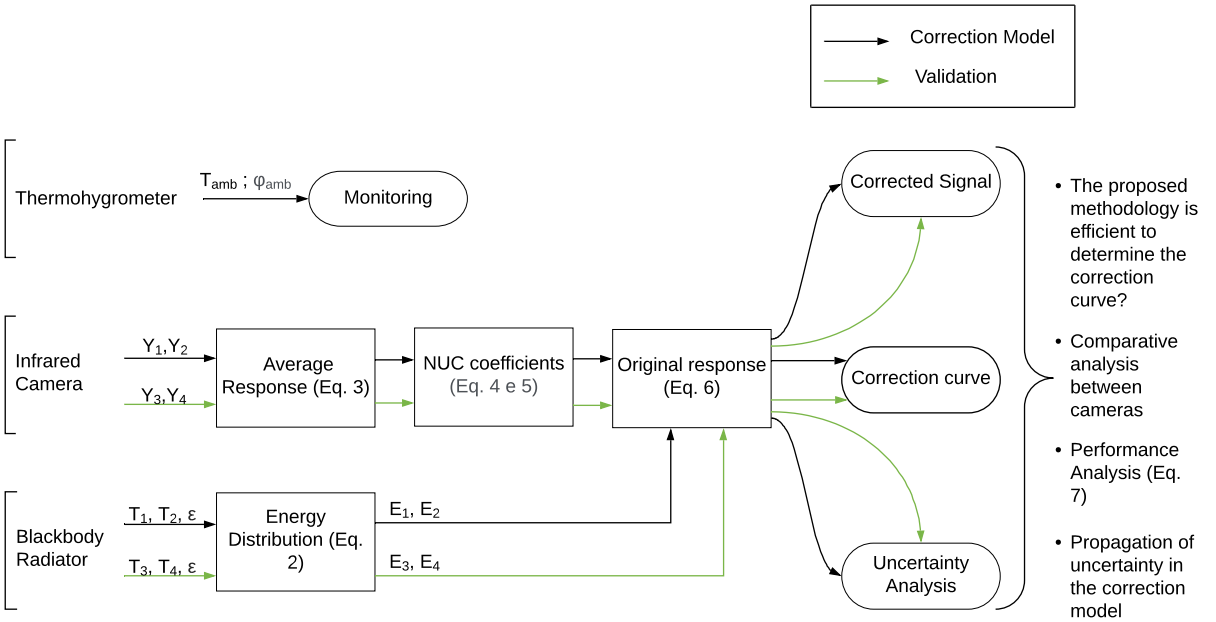

Figure 2: Diagram of the proposed methodology.

where ϵ_{obj} is the blackbody emissivity, τ is the atmospheric transmissivity and S_{obj}, S_{refl} and S_{atm} are the detector's inputs described by Planck's Law of blackbody radiation. In this study, the distance between the camera and the blackbody radiator is 5 cm, so the atmospheric transmissivity τ is considered to be unitary.

The global average (Eq. 3) of the detector's response is determined for each reference point. These values will be used to calculate the correction coefficients.

$$\bar{Y} = \frac{1}{MN} \sum_{i=1}^{M} \sum_{j=1}^{N} Y_{ij} \tag{3}$$

where M and N represent the digital resolution of the thermal camera.

The corrected gain and offset are then calculated with the global average and raw response in each reference point, according to Eq. 4 and Eq. 5, respectively.

$$G_{ij} = \frac{\bar{Y}(T_2) - \bar{Y}(T_1)}{Y_{ij}(T_2) - Y_{ij}(T_1)} \tag{4}$$

$$O_{ij} = \bar{Y}(T_2) - G_{ij} Y_{ij}(T_2) \tag{5}$$

where $\bar{Y}(T_2)$ is the global average of detector's response for T_2, $\bar{Y}(T_1)$ is the global average of detector's response for T_1, $Y_{ij}(T_2)$ is the digital signal for T_2, $Y_{ij}(T_1)$ is the digital signal for T_1. The corrected response for each pixel is determined by applying the coefficients into the original response. The corrected response is then obtained by Eq. 6.

$$Y_{c_{ij}} = G_{ij} Y_{ij} + O_{ij} \tag{6}$$

To evaluate the performance of the NUC model, the statistical parameter normalized root-mean square error is used. It describes the residual non-uniformity (RNU) in the detector's response by analyzing the standard deviation normalized by the average response, according to Eq. 7.

$$RNU = \frac{1}{\bar{Y}} \sqrt{\frac{1}{MN} \sum_{i=1}^{M} \sum_{j=1}^{N} \left[Y_{ij} - \bar{Y} \right]^2} * 100 \tag{7}$$

3.2 Experimental Procedure

The experimental procedure were carried to obtain the digital signal for each reference point set on the blackbody radiator. The reference temperatures were monitored by a T-type thermocouple calibrated by procedures to approximate the International Temperature Scale (BIPM, 1997) and the data acquisition system NI 9211 Series C. The ambient conditions

(temperature and humidity) were monitored by the digital thermo-hygrometer Testo 622 with an uncertainty of $\pm$ 0.4 ^oC and $\pm$ 3 %, respectively. The thermal cameras used in the experimental procedure were the PANASONIC AMG8833 FPA with an operational range of 0 ^oC to 80 ^oC and an uncertainty of $\pm$ 2.5 ^oC. The digital resolution of the imagers is 8x8 pixels and the wavelength of operation of 5 μm to 13 μm. A FLUKE 4181 extended area blackbody radiator was used to provide the uniform source of radiation. The operational range of the blackbody is 30 ^oC to 500 ^oC and its emissivity is 0.95.

Each camera was placed in front of the blackbody radiator, both positioned in supports to ensure the alignment, with a distance of 5 cm so that the field of view of the camera was inserted in the emission area. The ambient temperature was maintained between 18 ^oC and 20 ^oC and the humidity between 30 % and 40 %. The correction points set on the blackbody radiator were 30 ^oC and 45 ^oC and for each temperature, the array of digital signal was collected by the camera. In the validation procedure, the temperatures of 35 ^oC and 40 ^oC were analyzed. For each temperature, 10 different arrays were collected and then averaged to minimize temporal error. Figure 3 illustrates the experimental procedure.

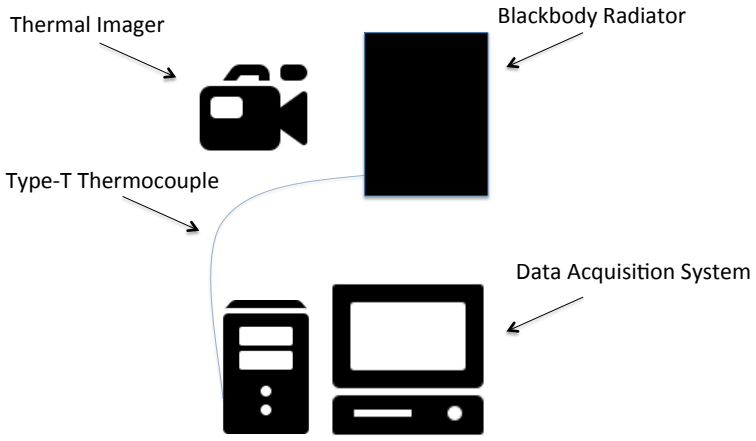

Figure 3: Sketch of the experimental procedure.

3.3 Uncertainties Propagation

In order to determine the uncertainties propagation in the proposed methodology, we followed the guidelines outlined in the Guide to the Expression of Uncertainty in Measurement (JCGM:100, 2008). In this model, the evaluation of uncertainties is a complex and essential analysis. Every detector of the focal plane array is an independent sensor, with its own singularities (i.e., responsiveness, noise, correction coefficients) so the uncertainty analysis is made pixel-by-pixel. First, it is necessary to categorize each input component in the uncertainty model, treating them individually, unless there is some correlation between variables. Each uncertainty component is treated either as a Type A or Type B variable. Type A evaluation is determined from the standard deviation, obtained by the measurement procedure and Type B components are determined from manufactures data and previous analysis.

To fully categorize the expanded uncertainty in the proposed model, we accounted the uncertainties since the experimental procedure up to the mathematical model of correction used to determine the corrected response. The uncertainty budget is then divided into three groups: blackbody radiator, thermal imager and mathematical model of correction. The uncertainty components are fully described in Table 1. The uncertainties related to the blackbody radiator were obtained by the manufacturer FLUKE (FLUKE, 2013; Liebmann, 2008) and are all dependent on the reference temperature.

As previous mentioned in the Experimental Procedure subsection, the temperature of the blackbody radiator is indicated by a T-type thermocouple, calibrated with procedures for approximating the International Temperature Scale, ITS-90 (BIPM, 1997). Therefore, the standard uncertainty component u_4 was obtained by the calibration procedure.

The uncertainty related to the temperature resolution, u_6, indicates the influence of the limited resolution of the thermal imager to detect a minimum temperature difference in the observed scene. Since this component is associated to

Table 1: Uncertainty components assumed for the proposed methodology.

Uncertainty Source	Component	Distribution	Characterization
Blackbody Radiator			
Stability	u_1	Uniform	Manufactures data
Uniformity	u_2	Uniform	Manufactures data
Emissivity	u_3	Normal	Manufactures data
Temperature Indication	u_4	Normal	Measured
Heat Loss	u_5	Normal	Manufactures data
Thermal Imager			
Temperature Resolution	u_6	Uniform	Measured
Standard Deviation	u_7	Normal	Measured
Correction Model			
Mathematical Model (NUC)	u_8	Normal	Measured

characteristics of the camera, they are constant for the whole analyzed range. The temperature resolution (TR) can be estimated by Eq. 8 (Chrzanowski, 2001).

$$TR = \frac{\Delta T_{span}}{2^k} \tag{8}$$

where ΔT_{span} is the temperature range of the imager and k is the resolution of the A/D converter, in bits. The uncertainty u_6 is assumed to have a uniform distribution and it is given by Eq. 9.

$$u_6 = \frac{TR}{\sqrt{12}} \tag{9}$$

Standard deviation uncertainty is related to the drift in response given by each detector between frames, under the same experimental conditions. The estimation of the component is given by the experimental standard deviation, s, determined by Eq. 10 and the uncertainty u_7 is calculated by Eq. 11.

$$s = \sqrt{\frac{1}{N-1}\sum_{j=1}^{N}\left(Y_j - \bar{Y}\right)^2} \tag{10}$$

$$u_7 = \frac{s}{\sqrt{N}} \tag{11}$$

where N is the number of frames, Y_j is the detector response in each frame and $\bar{Y}$ is the average detector response between frames.

The standard uncertainty of the mathematical model, u_8, was obtained by analyzing the model for corrected response, given by Eq. 6. To determine the uncertainty of the mathematical model, a correlation between G_{ij} and O_{ij} coefficients was considered and the contribution of each variable to the model was determined. The estimated correlation coefficient between the two variables is determined by Eq. 12 and the standard uncertainty u_8 is given by Eq. 13 (Albetazi and Souza, 2018).

$$r\left(G,O\right) = \frac{\sum_{i=1}^{N}\left(G_i - \bar{G}\right)\left(O_i - \bar{O}\right)}{\sqrt{\sum_{i=1}^{N}\left(G_i - \bar{G}\right)^2 \sum_{i=1}^{N}\left(O_i - \bar{O}\right)^2}} \tag{12}$$

$$u_8 = \sqrt{\sum_{i=1}^{N}\left(\frac{\partial f}{\partial X_i}\right)^2 u^2\left(X_i\right) + 2\sum_{i=1}^{N}\sum_{j=1}^{N}\frac{\partial f}{\partial X_i}\frac{\partial f}{\partial X_j}u\left(X_i\right)u\left(X_j\right)r\left(X_i,X_j\right)} \tag{13}$$

where f is the mathematical model, $\left(\frac{\partial f}{\partial X_i}\right)$ is the partial derivative of the function f related to the input variable X_i and $\mathrm{u}(X_i)$ is the standard uncertainty of the input variables.

The propagated standard uncertainty is obtained by combining the standard uncertainty of each of the input components depicted in Table 1. Assuming that there is no correlation between the components, the propagated combined uncertainty, u_c, is determined by Eq. 14.

$$u_c = \sqrt{\sum_{i=1}^{N}\left(\frac{\partial f}{\partial u_i}\right)^2 u_i^2} \tag{14}$$

The coverage factor k_p is determined on the basis of the t-distribution with an effective degree of freedom of the model, ν_{eff}, that is given by the Eq. 15 (JCGM:100, 2008). The confidence level p determined for the interval is obtained by the approximation $k_p = t_p(\nu_{eff})$.

$$\nu_{eff} = \frac{u_c^4}{\sum_{i=1}^{N} \frac{u_i^4}{\nu_i}} \tag{15}$$

where u_c is the combined uncertainty, u_i is the standard uncertainty components and ν_i is the degree of freedom of each uncertainty component in the model. The expanded uncertainty, U (Eq. 16), is obtained by multiplying the combined standard uncertainty u_c by the coverage factor k_p to define the interval where the measurement result may be distributed.

$$U = k_p u_c \tag{16}$$

4. RESULTS

4.1 Evaluation of the NUC model

We inspected the cameras over the range of approximately 30 ^oC to 45 ^oC with a 5 ^oC interval and the two-points set on the blackbody radiator for the correction were T_{bb_1} = 30 ^oC and T_{bb_2} = 45 ^oC. Figure 4 shows the correction curve for the three cameras along with the uncorrected response of two pixels for comparison. The corrected signal response was obtained by applying the correction coefficients (Eq. 4 and Eq. 5) into the original response. It is important to point out that there is only one array of gain and offset coefficients for the whole inspected range. Since these coefficients are obtained using the responses of the two reference points, the correction is theoretically perfect for them, but it degrades in between the interval.

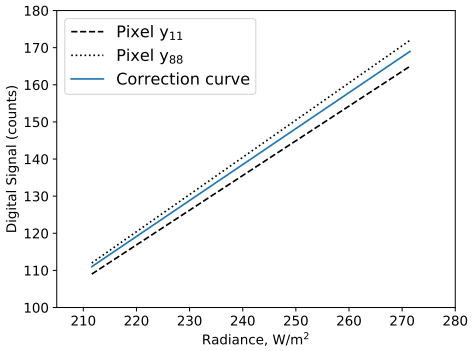

(a) Thermal camera 1

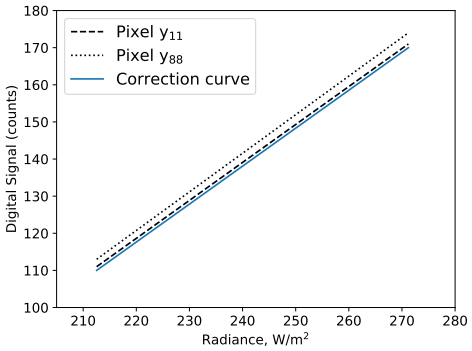

(b) Thermal camera 2

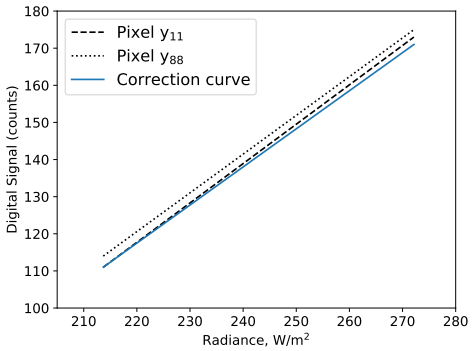

(c) Thermal camera 3

Figure 4: Correction curves for the inspected cameras.

Figure 5 shows the residual non-uniformity (Eq. 7) obtained for the raw data and the corrected response by the NUC model for each camera. As shown in the NUC model curves in Fig. 5, the standard deviation in the correction points for all cameras is zero, which indicates that all pixels have the same response, equal to the average of the original response. As the temperature moves away from the correction points, the standard deviation increases, but it is clear that the correction is efficient to reduce the spatial noise. Residual non-uniformity dropped from 1.00 % on average to 0.16 % in CAM 1, 0.88 % to 0.15 % in CAM 2 and 0.94 % to 0.18 % in CAM 3 applying the proposed NUC model over the inspected range.

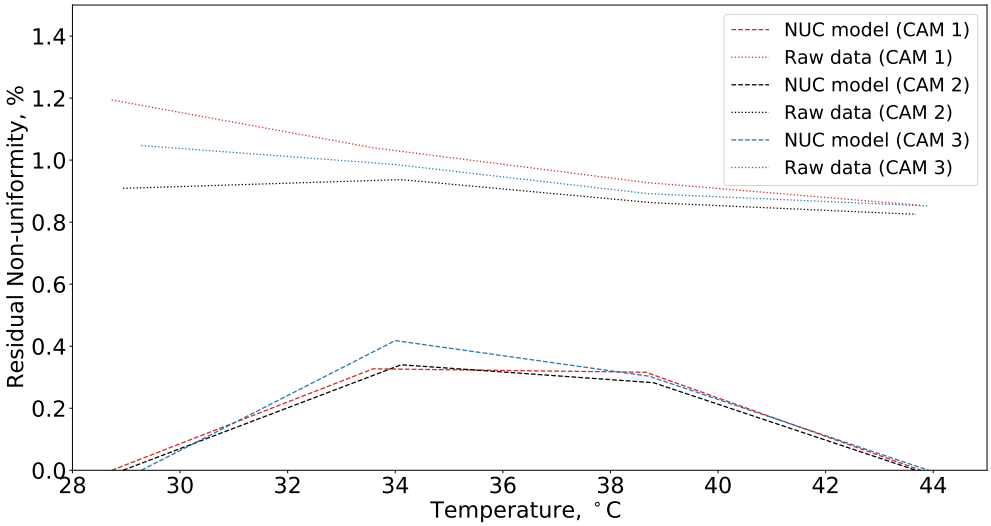

Figure 5: Residual non-uniformity for raw data and NUC model.

In order to examine the proximity of the corrected response to the reference temperature (T_{ref}) indicated by the thermocouple placed on the blackbody, we converted the corrected response into temperature (T_{nuc}) over the analyzed range. Figure 6 shows the deviation between the corrected temperature from the NUC model and the reference temperature in the blackbody radiator. This deviation occurs in every inspected camera and it is an intrinsic characteristic of the NUC methodology. The corrected response is determined by individual gain and offsets to standardize the response of detectors and does not take into account a relation to the reference temperature. To obtain a radiometric correction, a relationship between reference temperature and corrected signal is required.

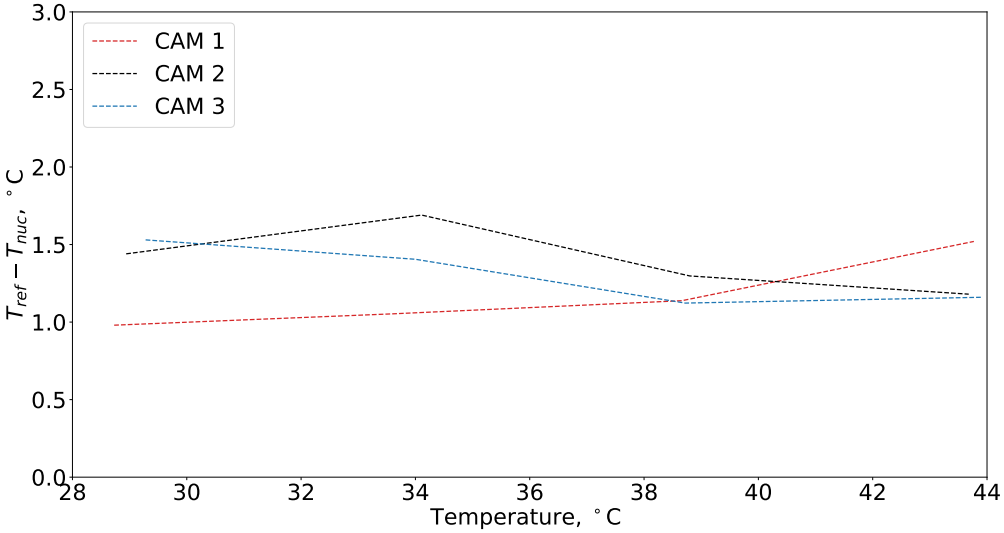

Figure 6: Deviation between the reference temperature and corrected temperature from NUC model.

4.2 Uncertainty Propagation

Tables 2, 3 and 4 shows the uncertainty budget for the inspected cameras. Since the uncertainties related to the standard deviation and the mathematical model along with the combined and expanded uncertainties are obtained for each individual detector, we display the values for the pixel with the highest uncertainty in the FPA. The uncertainties related to the blackbody radiator are all dependent on the reference temperature making them almost identical in all cameras. It is possible to verify that the highest contribution to the expanded uncertainty in all cameras is the component u_4, associated with the indication of reference temperature, accounting up to 59 % of the overall value. The component related to the

standard deviation is the second highest source of uncertainty, adding up to 20 % of the expanded uncertainty, followed by the stability and correction model accounting up to 9.5 % and 6 %, respectively.

Table 2: Uncertainty budget for Camera 1.

Uncertainty Source	Comp.	Distr.	Uncertainty (CAM 1), ^oC				ν
Blackbody Radiator			**28.73** ^oC	**33.59** ^oC	**38.66** ^oC	**43.77** ^oC	
Stability	u_1	Uniform	0.067	0.069	0.072	0.074	∞
Uniformity	u_2	Uniform	0.011	0.012	0.012	0.013	∞
Emissivity	u_3	Normal	0.009	0.014	0.019	0.024	∞
Temperature Indication	u_4	Normal	0.427	0.426	0.424	0.423	∞
Heat Loss	u_5	Normal	0.001	0.002	0.004	0.005	∞
Thermal Imager							
Temperature Resolution	u_6	Uniform	0.006	0.006	0.006	0.006	∞
Standard Deviation	u_7	Normal	0.147	0.129	0.112	0.132	9
Correction Model							
Mathematical Model (NUC)	u_8	Normal	0.041	0.036	0.033	0.041	∞
Combined Uncertainty	u_c	Normal (k = 1)	0.459	0.452	0.446	0.452	∞
Expanded Uncertainty	U	Normal (k = 2)	0.918	0.905	0.893	0.904	

Table 3: Uncertainty budget for Camera 2.

Uncertainty Source	Comp.	Distr.	Uncertainty (CAM 2), ^oC				ν
Blackbody Radiator			**28.95** ^oC	**34.11** ^oC	**38.81** ^oC	**43.68** ^oC	
Stability	u_1	Uniform	0.067	0.069	0.072	0.074	∞
Uniformity	u_2	Uniform	0.012	0.012	0.013	0.013	∞
Emissivity	u_3	Normal	0.009	0.015	0.019	0.024	∞
Temperature Indication	u_4	Normal	0.427	0.426	0.424	0.423	∞
Heat Loss	u_5	Normal	0.002	0.003	0.004	0.005	∞
Thermal Imager							
Temperature Resolution	u_6	Uniform	0.006	0.006	0.006	0.006	∞
Standard Deviation	u_7	Normal	0.132	0.126	0.108	0.097	9
Correction Model							
Mathematical Model (NUC)	u_8	Normal	0.036	0.033	0.031	0.032	∞
Combined Uncertainty	u_c	Normal (k = 1)	0.454	0.451	0.446	0.442	∞
Expanded Uncertainty	U	Normal (k = 2)	0.908	0.903	0.892	0.885	

Table 4: Uncertainty budget for Camera 3.

Uncertainty Source	Comp.	Distr.	Uncertainty (CAM 3), ^oC				ν
Blackbody Radiator			**29.28** ^oC	**34.00** ^oC	**38.72** ^oC	**43.91** ^oC	
Stability	u_1	Uniform	0.067	0.069	0.072	0.074	∞
Uniformity	u_2	Uniform	0.012	0.012	0.013	0.013	∞
Emissivity	u_3	Normal	0.009	0.015	0.019	0.024	∞
Temperature Indication	u_4	Normal	0.427	0.426	0.424	0.423	∞
Heat Loss	u_5	Normal	0.002	0.003	0.004	0.005	∞
Thermal Imager							
Temperature Resolution	u_6	Uniform	0.006	0.006	0.006	0.006	∞
Standard Deviation	u_7	Normal	0.118	0.118	0.112	0.118	9
Correction Model							
Mathematical Model (NUC)	u_8	Normal	0.031	0.032	0.029	0.035	∞
Combined Uncertainty	u_c	Normal (k = 1)	0.449	0.449	0.446	0.448	∞
Expanded Uncertainty	U	Normal (k = 2)	0.899	0.898	0.893	0.895	

Considering that the uncertainty propagation in this model is made pixel-by-pixel, we created a thermal map for each reference temperature, Fig. 7, with the distribution of expanded uncertainties among pixels. Taking into account that the thermal maps for all cameras exhibits the same pattern, we present only the visualization for Camera 3. It can be seen in Figs. 7a, 7b, 7c and 7d that the uncertainties are not uniformly distributed among detectors and they vary greatly between reference temperatures. This behavior can be explained by the nature of thermal detectors that have individual responsiveness along with particular correction coefficients and noises. Although the highest contribution to the expanded uncertainty belongs to the reference temperature as it shapes up to 59 % of the total value, the span of uncertainty values among pixels is relatively small, so the contributions related to the standard deviation and correction model, which are made pixel-by-pixel, have a strong influence on the pattern exhibited in Fig. 7.

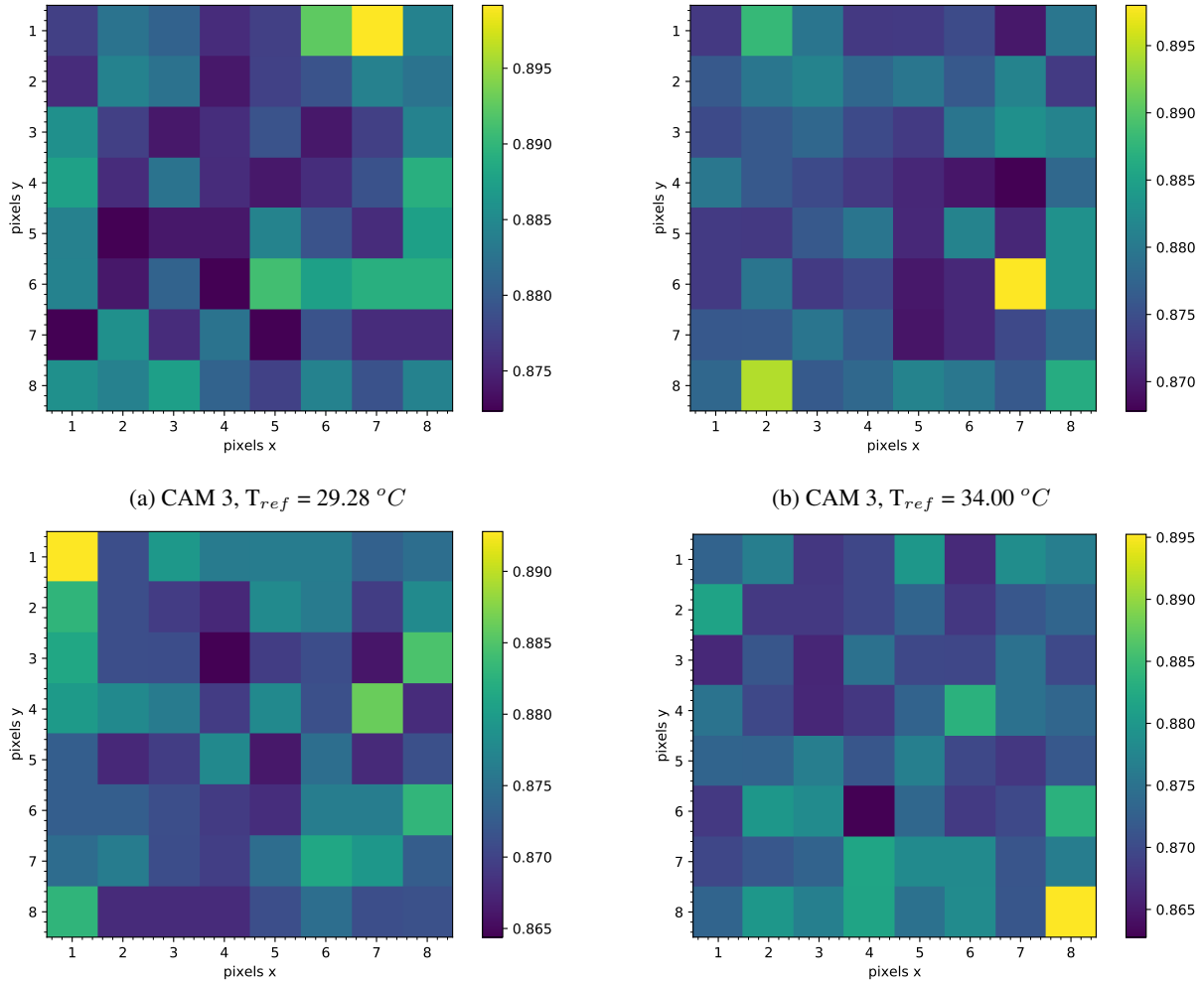

(a) CAM 3, T_{ref} = 29.28 ^oC

(b) CAM 3, T_{ref} = 34.00 ^oC

(c) CAM 3, T_{ref} = 38.72 ^oC

(d) CAM 3, T_{ref} = 43.91 ^oC

Figure 7: Distribution of uncertainties in the FPA for Camera 3.

5. CONCLUSION

In this article, we evaluated thermal camera's non-uniformity correction on the basis of performance and accuracy. In order to provide an uncertainty analysis for the traditional correction, we applied the guidelines of the Guide to the Expression of Uncertainty in Measurement (JCGM:100, 2008).

To obtain the raw responses of the inspected thermal imagers, an experimental bench was mounted and we collected the digital signal in each reference point set on the blackbody radiator. The two-point NUC methodology was applied in the original response to obtain the correction coefficients and corrected response. We could conclude that the traditional two-point NUC methodology is an efficient way to reduce spatial noise among detectors but only if applied in a narrow range of operation. This is due to residual spatial noise that remains in the corrected responses outside the correction points.

Considering that the correction is based on the average of response, if a camera has an expressive spatial noise among detectors, the correction will be further from the reference set points. Additionally, it can be concluded that despite being

an efficient method for mitigating spatial noise in thermal imagers, the NUC technique does not necessarily provide a radiometric correction. It is important to distinguish a calibration procedure from a correction procedure. The NUC method should be implemented in a calibration scheme with a radiometric adjustment, approximating the corrected signal to the reference temperature.

In the uncertainty propagation model, we accounted the components since the experimental procedure up to the NUC model for correction. The uncertainties related to the blackbody radiator were dominant in the uncertainty model, especially the indication of reference temperature. Standard deviation and correction model components also exhibit a great influence on the distribution of the expanded uncertainty, as can be seen in Fig. 7. The cameras inspected on this study have a narrow operation range, low resolution and some technical details of operation are not provided by the manufacturer. In order to fully evaluate the accuracy of the proposed correction model, the thermal imager should be extensively characterized, including uncertainties from the spectral response, intrinsic errors and detector's self emission.

6. ACKNOWLEDGMENTS

This study was financed in part by CAPES (Coordenação de Aperfeiçoamento de Pessoal de Nível Superior), the CNPq (Conselho Nacional de Desenvolvimento Científico e Tecnológico - Brazil), and by the PRPq (Pró-Reitoria de Pesquisa da Universidade Federal de Minas Gerais).

7. REFERENCES

Albetazi, A. and Souza, A., 2018. *Fundamentos de Metrologia Científica e Industrial*. Manole, 2nd edition.

BIPM, 1997. "Techniques for approximating the international temperature scale of 1990". Technical report.

Chang, S. and Li, Z., 2019. "Single-reference-based solution for two-point non-uniformity correction of infrared focal plane arrays". *Infrared Physics and Technology*, Vol. 101, pp. 96–104.

Chrzanowski, K., 2001. "Evaluation of thermal cameras in quality systems according to iso 9000 or en45000 standards". *Proc. SPIE*, Vol. 4360, pp. 387–401.

FLUKE, 2013. "4181 precision infrared calibrator technical guide". Technical report.

Honorat, V., Moreau, S., Muracciole, J., Wattrisse, B. and Chrysochoos, A., 2005. "Calorimetric analysis of polymer behaviour using a pixel calibration of an irfpa camera". *Quantitative Infrared Thermography Journal*, Vol. 22, pp. 153–171.

JCGM:100, 2008. "Evaluation of measurement data - guide to the expression of uncertainty in measurement". Technical report.

Li, Z., Yu, Y., Tian, Q.J., Chang, S.T., He, F.Y., Yin, Y.H. and Qiao, Y.F., 2017. "High-efficiency non-uniformity correction for wide dynamic linear infrared radiometry system". *Infrared Physics and Technology*, Vol. 85, pp. 395–402.

Liebmann, F., 2008. "Infrared calibration development at fluke corporation hart scientific division". In *Proceedings of the 16th CALCON Technical Conference*. Utah, USA.

Machin, G., Simpson, R. and Broussely, M., 2008. "Calibration and validation of thermal imagers". *Quantitative Infrared Thermography*, Vol. 7, pp. 133–147.

Miao, L.F., Xu, Q., Zhang, M., Sun, D. and Liu, Y., 2009. "Real-time implementation of multi-point non-uniformity correction for irfpa based on fpga". *International Symposium on Photoelectronic Detection and Imaging*, Vol. 2, pp. 5–15.

Nelson, M.D., Johnson, J.F. and Lomheim, T.S., 1991. "General noise processes in hybrid infrared focal plane arrays". *Optical Engineering*, Vol. 30, pp. 1682–1700.

NISTIR, 2015. "Calibration and measurement procedures for a high magnification thermal camera". Technical report.

Poncelet, M. and Witz, J.F.S., 2011. "A study of irfpa camera measurement errors: Radiometric artefacts". *Quantitative Infrared Thermography Journal*, Vol. 8, pp. 165–186.

Redlich, R., Figueroa, M., Torres, S. and Pezoa, J., 2015. "Embedded non-uniformity correction in infrared focal plane arrays using the constant range algorithm". *Infrared Physics and Technology*, Vol. 69, pp. 164–173.

Rui, L., Tang, Y.Y., Qing, L. and Xin, Z., 2009. "Improvement in adaptive non-uniformity correction method with nonlinear model for infrared focal plane arrays". *Optics Communications*, Vol. 282, pp. 3444–3447.

Saux, V.L. and Doudard, C., 2016. "Proposition of a compensated pixelwise calibration for photonic infrared cameras and comparison to classic calibration procedures: Case of thermoelastic stress analysis". *Infrared Physics and Technology*, Vol. 80, pp. 83–92.

Zhou, H.X., Qin, H., Bai, L., Liu, Q., Geng, X. and Wang, B., 2009. "Non-uniformity correction algorithm with nonlinear model for infrared focal plane arrays". *Infrared Physics and Technology*, Vol. 53, pp. 10–16.

8. RESPONSIBILITY NOTICE

The authors are the only responsible for the printed material included in this paper.